

## Strong Universality and Algebraic Scaling in Two-Dimensional Ising Spin Glasses

T. Jörg,<sup>1</sup> J. Lukic,<sup>1</sup> E. Marinari,<sup>2</sup> and O. C. Martin<sup>3</sup>

<sup>1</sup>*Dipartimento di Fisica, Università di Roma “La Sapienza,” SMC and INFN, Piazzale Aldo Moro 2, 00185 Roma, Italy*

<sup>2</sup>*Dipartimento di Fisica, INFN, Università di Roma “La Sapienza,” Piazzale Aldo Moro 2, 00185 Roma, Italy*

<sup>3</sup>*Laboratoire de Physique Théorique et Modèles Statistiques, Bâtiment 100, Université Paris-Sud, F-91405 Orsay, France*

(Received 19 January 2006; published 16 June 2006)

At zero temperature, two-dimensional Ising spin glasses are known to fall into several universality classes. Here we consider the scaling at low but nonzero temperatures and provide numerical evidence that  $\eta \approx 0$  and  $\nu \approx 3.5$  in all cases, suggesting a unique universality class. This algebraic (as opposed to exponential) scaling holds, in particular, for the  $\pm J$  model, with or without dilutions, and for the plaquette diluted model. Such a picture, associated with an exceptional behavior at  $T = 0$ , is consistent with a real space renormalization group approach. We also explain how the scaling of the specific heat is compatible with the hyperscaling prediction.

DOI: 10.1103/PhysRevLett.96.237205

PACS numbers: 75.10.Nr, 64.60.Fr, 75.40.Mg, 75.50.Lk

*Introduction.*—Critical phenomena in disordered systems remain a severe challenge. In fact, many properties that are well established in pure systems (such as upper critical dimension, universality, etc.) are still open to debate when strong disorder is present. This is the case, in particular, for spin glasses (SG), i.e., magnetic systems incorporating both disorder and frustration [1].

In this Letter, we focus on two-dimensional SG because (i) they are computationally tractable, and (ii) their zero temperature ( $T = 0$ ) universality classes [2] are well established. For our purposes, there are two such  $T = 0$  classes, associated with whether or not all excitation energies are multiples of a given quantum. The corresponding spin-glass stiffness exponent  $\theta$  is zero in the first class (as in the  $\pm J$  model) and is close to  $-0.28$  in the second class (as when the couplings are Gaussian random variables). Following standard scaling arguments [3,4] to infer the finite  $T$  behavior, the thermal exponent should be given by  $\nu = -1/\theta$ ; when  $\theta = 0$ , formally  $\nu = \infty$  so that the correlation length  $\xi$  should diverge faster than any power of inverse temperature  $\beta = 1/T$  (e.g., exponential scaling). One’s expectation is then that the two universality classes defined at  $T = 0$  could have direct counterparts at  $T > 0$ .

Recent numerical work [5,6] has confirmed the relation  $\nu = -1/\theta$  in the case of Gaussian couplings; similarly, all of the latest works [7–10] on the  $\pm J$  model (for which  $\theta = 0$ ) have concluded that  $\nu = \infty$ . We reconsider here this issue in greater depth, comparing models with different distributions of spin-spin couplings, using advanced Monte Carlo and partition function solvers and applying sophisticated extrapolations to the infinite volume limit. In contrast with previous claims, we conclude that  $\xi(T)$  diverges with the same exponent  $\nu \approx 3.5$  for all considered models. Furthermore, we find that the exponent  $\eta$  also seems to be the same regardless of the details of the couplings. We are thus in a situation where the  $T > 0$  properties fall into *just one universality class*, whereas two classes arise when considering the  $T = 0$  properties (where the quantized nature of energies can be relevant). A

simple interpretation of this unusual phenomenon is that, at  $T = 0$ , one has an “additional” fixed point (realized only when energies are quantized), but that this fixed point is irrelevant for the critical properties defined just above  $T_c$ . We have also investigated the specific heat singularities of our models. Here we find a behavior that is asymptotically compatible with  $T_c = 0$  hyperscaling.

*Models, computational methods, and analysis.*—We consider the 2D Edwards-Anderson model defined by the Hamiltonian [11]

$$\mathcal{H} = -\sum_{\langle xy \rangle} J_{xy} \sigma_x \sigma_y, \quad (1)$$

where the sum is over all the nearest neighbor pairs of a 2D square lattice of length  $L$  with periodic boundary conditions. The  $\sigma_x = \pm 1$  are Ising spins. We take the couplings  $J_{xy}$  to be independent random variables, chosen from several distributions in order to check their effect on the critical behavior. In particular, we shall consider: (1) the  $\pm J$  model, where  $J_{xy} = \pm 1$  with equal probability; (2) the diluted  $\pm J$  model obtained from the undiluted case by setting a fraction  $(1 - p)$  of the couplings to zero; (3) the “irrational model,” where  $J_{xy} = \pm 1$  or  $\pm G$  with equal probability for these 4 values,  $G$  being the golden mean  $G = (1 - \sqrt{5})/2 \approx -0.618$ ; (4) a distribution with  $\frac{1}{2}$  of the couplings equal to  $\pm 1$  and one-half equal to  $\pm \frac{1}{4}$ : We call it the “gap 1/4” model.

We tackled these systems using two complementary approaches. First, we applied cluster replica Monte Carlo along with parallel tempering and numerous algorithmic optimizations [8,12,13]; such an approach can provide high quality estimates of configurational averages even for large lattices. Second, we used exact partition function computations [14], which give us the value of the free energy and specific heat for individual samples at arbitrary temperatures. In all cases, for each lattice size  $L$ , we used a large number of disorder realizations for each of the distributions mentioned previously; typically, we used thou-

sands of such samples. In spite of the large lattices sizes we are able to handle, it is appropriate to use sophisticated techniques for analyzing the effects of finite  $L$ . Starting with a suitably defined finite-volume correlation length  $\xi(T, L)$  (see later) and a long-range observable  $\mathcal{O}(T, L)$  such as the spin-glass susceptibility  $\chi_{\text{SG}}(T, L)$ , finite size scaling (FSS) theory predicts

$$\frac{\mathcal{O}(T, sL)}{\mathcal{O}(T, L)} = F_{\mathcal{O}}(\xi(T, L)/L; s) + O(\xi^{-\omega}, L^{-\omega}). \quad (2)$$

Here  $F_{\mathcal{O}}$  is the FSS function and  $s > 1$  is a scale factor. Equation (2) is an excellent starting point for investigations of the FSS behavior, as it involves only finite-volume quantities taken from a pair of systems with sizes  $L$  and  $sL$  at a given  $T$ . The knowledge of the scaling functions  $F_{\mathcal{O}}$  (where  $\mathcal{O}$  is, in our case,  $\chi_{\text{SG}}$ ) and  $F_{\xi}$  (where  $\mathcal{O}$  is  $\xi$ ) allows us to extract information on the critical behavior using an infinite volume extrapolation [15,16]. This technique works with data strictly above  $T_c$  and, hence, is well suited to our case for which  $T_c = 0$ . In essence, it uses  $F_{\xi}$  and  $F_{\mathcal{O}}$  to obtain the thermodynamic limit of  $\mathcal{O}$  using an iterative procedure in which the pair  $\xi$  and  $\mathcal{O}$  is scaled up from  $L \rightarrow sL \rightarrow s^2L \rightarrow \dots \rightarrow \infty$  as described in Ref. [15]. Detailed knowledge of the critical behavior can then be obtained from appropriate fits to the extrapolated data. To show that this relatively sophisticated technique works well in our system, we display in Fig. 1 the FSS function  $F_{\xi}$  determined from these procedures, for several of our models. The excellent data collapse at small values of  $\xi/L$  ( $\xi/L < 0.45$ ) (already noticed in Refs. [17,18]) validates the FSS framework. Furthermore, we see that these FSS functions are independent of the distribution of couplings  $J_{xy}$ ; that is precisely what should transpire if there is a single universality class in our system. The region of the excellent data collapse increases with the size of the system, suggesting

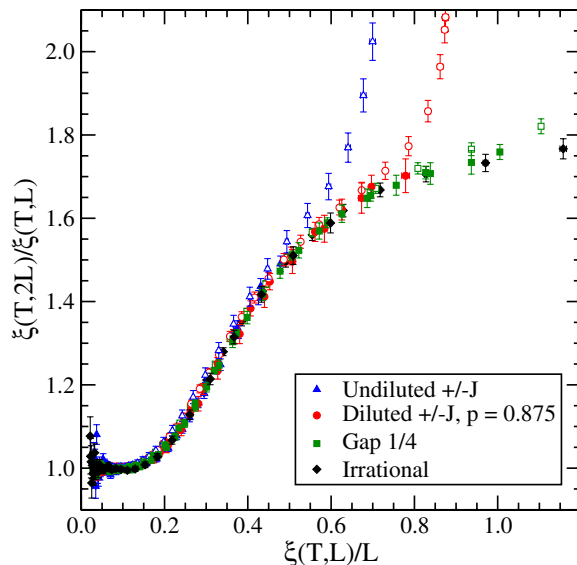


FIG. 1 (color online). The FSS function  $F_{\xi}$ .

strongly a single limiting FSS function. The diluted and the gap 1/4 model are the most important pieces of evidence on which our conclusions rest. The diluted model has smaller finite size effects than the undiluted one: This allows us to go to very reliable extrapolations. We have been able to thermalize systems up to  $L = 64$  (with 2000 samples).

*The spin-glass susceptibility and the exponent  $\eta$ .*—In our Monte Carlo simulations, we follow two replicas from which we can measure the local spin overlaps  $q_x = \sigma_x^{(1)} \sigma_x^{(2)}$  (the superscript is the replica index). Of interest is the two site correlation function of these overlaps; we define, in fact, the wave-vector-dependent spin-glass susceptibility via

$$\chi_{\text{SG}}(\vec{k}) = \frac{1}{L^2} \sum_{\vec{r}_1} \sum_{\vec{r}_2} e^{i\vec{k} \cdot (\vec{r}_2 - \vec{r}_1)} [\langle q_{\vec{r}_1} q_{\vec{r}_2} \rangle_{\text{T}}]_{\text{av}}. \quad (3)$$

The usual spin-glass susceptibility is then defined through  $\chi_{\text{SG}}(T, L) = L^2 \langle q^2 \rangle = \chi_{\text{SG}}(\vec{k} = \vec{0})$ . (We denote the thermal average at temperature  $T$  by  $\langle \cdot \cdot \cdot \rangle_{\text{T}}$  and the average over the disorder realizations by  $[\cdot \cdot \cdot]_{\text{av}}$ .)

The spin-glass susceptibility is a measure of the correlation volume of our system; using the standard form for a correlation function near a critical point

$$G(r) = \frac{e^{-r/\xi}}{r^{D-2+\eta}}, \quad (4)$$

we see that in  $D = 2$  as  $T \rightarrow 0$   $\chi_{\text{SG}}$  should behave as  $\chi_{\text{SG}} \sim \xi^{2-\eta}$ . To check this, we use our infinite volume extrapolations for both  $\xi(T)$  and  $\chi_{\text{SG}}(T)$  and display one versus the other in Fig. 2. It is remarkable that the data for our models fall on the same curve, indicating, in particular, that they all have the same exponent  $\eta$ , a highly surprising

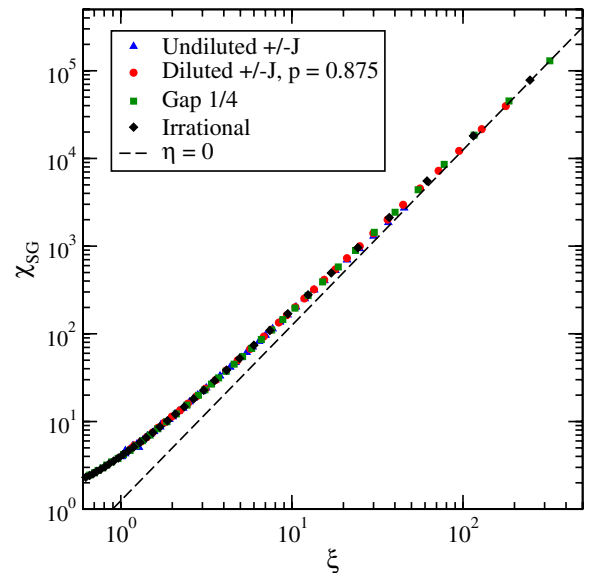


FIG. 2 (color online). Parameter-free plot of  $\chi_{\text{SG}}(T, \infty)$  versus  $\xi(T, \infty)$  for different coupling distributions. The line is for  $\eta = 0$ .

fact if there were two universality classes. Fits of this curve lead to values of  $\eta$  that are very small, between 0 and 0.1, strongly suggestive of  $\eta = 0$ ; note that one expects the models with continuous couplings to have  $\eta = 0$  exactly.

*The correlation length and the exponent  $\nu$ .*—The second moment of the overlap correlation function can be identified with the square of the correlation length. In practice, we define this length via

$$\xi(T, L) = \frac{1}{2 \sin(k_{\min}/2)} \left[ \frac{\chi_{\text{SG}}(0)}{\chi_{\text{SG}}(k_{\min})} - 1 \right]^{1/2}, \quad (5)$$

where  $\chi_{\text{SG}}$  is defined in Eq. (3). Note that  $k_{\min} = 2\pi/L$  is the modulus of the smallest nonzero wave vector allowed by periodic boundary conditions. We use our analysis methods to extract the large  $L$  limit of  $\xi(T, L)$ . Having done so for our different models, we find that their temperature dependence is not so different. This is illustrated in Fig. 3; we also see that the different models lead to rather parallel asymptotes, suggesting that the exponent  $\nu$  is the same for all of them. Analogous plots on a semilog scale do not give evidence for an exponential scaling of  $\xi$ , even for the  $\pm J$  model. Finally, performing power fits, we find values of  $\nu$  close to 3.5. Again, this goes in the direction of a single universality class.

*The specific heat and the exponent  $\alpha$ .*—We measured the specific heat density  $c_v$  via both Monte Carlo and the exact partition function techniques. In contrast to what was observed for  $\chi$  and  $\xi$ , the  $\pm J$  model and its diluted versions differ from the continuous models when one considers the very low  $T$  behavior of  $c_v$ . In the first class of models,  $c_v$  decreases fast as one approaches  $T = 0$ , while in the second class  $c_v$  looks linear in  $T$ . According to hyperscaling, when  $T_c = 0$ , one has the relation [19]

$$c_v(T) \sim T^{-\alpha} \quad \text{with } \alpha = -2\nu. \quad (6)$$

We saw that  $\nu \approx 3.5$ , so we expect  $\alpha \approx -7$ . The deceptive

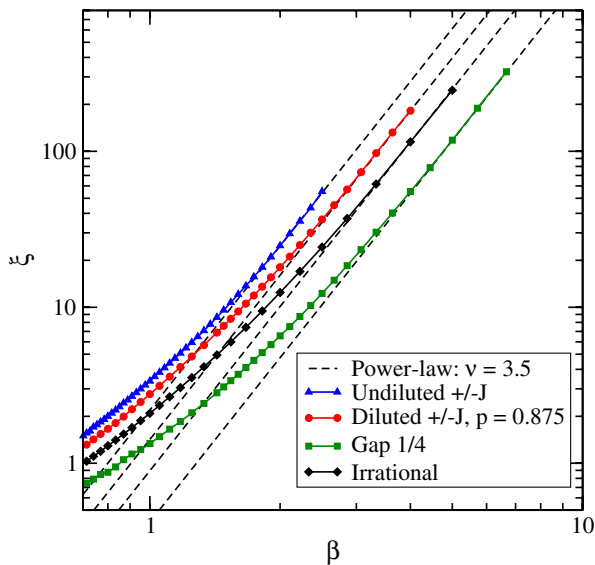


FIG. 3 (color online).  $\xi(\beta, \infty)$  as a function of  $\beta$ .

linear behavior in the continuous model can be easily understood. In the ground state of a continuous model, the local field on a spin is a continuous variable with a finite density at 0. Thus, at any low temperature, a fraction proportional to  $T$  of the system’s spins can be thermally activated, thereby leading to a linear dependence of  $c_v$  in  $T$ . The point is that the exponent  $\alpha$  describes the non-analytic scaling of  $c_v$ , but one can also have regular parts, namely, linear, quadratic, etc., in  $T$ . Since  $-\alpha$  is large, the nonanalytic part is subdominant compared to the analytic contributions and, thus, numerically invisible. The conclusion is that the continuous models make it impossible in practice to estimate  $\alpha$ . Fortunately, the situation is completely different for the  $\pm J$  model and its variants. There the leading analytic contribution to  $c_v$  is of the form  $T^{-2} \exp(-4J/T)$ , because the local field on any spin is a multiple of  $2J$ . This is far smaller than the predicted non-analytic term (a power of  $T$ ), so we are able to use these models to estimate  $\alpha$ . In Fig. 4, we show the specific heat of the  $\pm J$  model versus  $T$ . In the inset, we show the semilogarithmic plot of  $c_v$  to test for exponential scaling. The data are not compatible with an exponential scaling (the  $L = 80$  data are crucial to reach this conclusion), while an asymptotic power law behavior is consistent with the data and with the hyperscaling of Eq. (6). 2D disordered systems with different choices of a (frustrated) disorder behave in the same way [20], making our claim about a strong universality even stronger.

*A renormalization group justification.*—In the picture we are proposing, the thermal properties ( $T > 0$ ) of 2D SG fall into just one universality class, in contrast to the properties defined at exactly  $T = 0$ . Furthermore, the relation  $\nu = -1/\theta$  holds if we take  $\theta$  from the  $T = 0$  class of “continuous models” (where  $\theta$  is nonzero). We are thus faced with a situation where continuous models behave as expected, but the  $\pm J$  models have (i) a separate (exceptional) behavior at  $T = 0$  and (ii) fall into the continuous class when  $T > 0$ . To justify theoretically this scenario, we appeal to a real space renormalization group (RG) framework. Consider the Migdal-Kadanoff (MK) construction

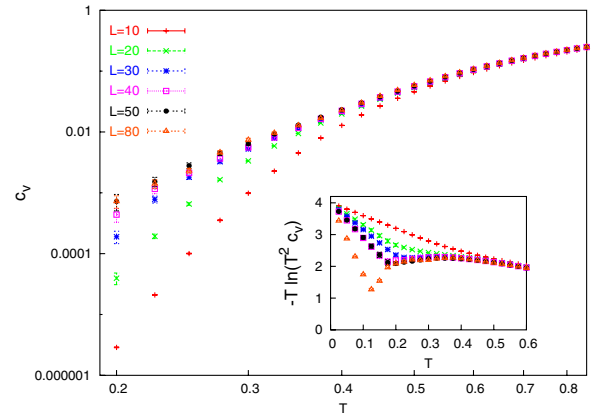


FIG. 4 (color online). Specific heat of the  $\pm J$  model versus  $T$  in a log-log plot. Inset: Plot of  $-T \ln(T^2 c_v)$  versus  $T$ .

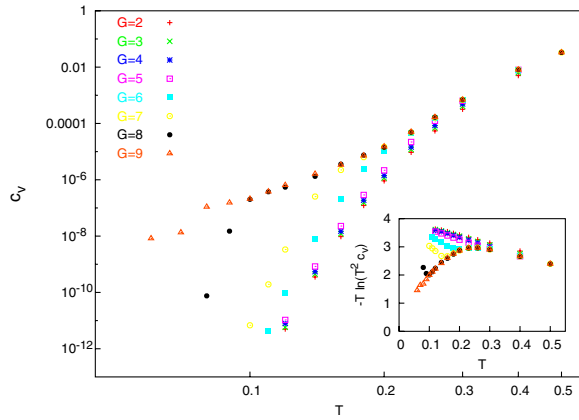


FIG. 5 (color online). Specific heat for the  $\pm J$  model on MK lattices versus  $T$  in a log-log display.  $G$  is the number of recursions of the MK construction. Inset: The same data but for a semilog display, which should be straight in the case of exponential scaling.

for spin glasses [21]. These hierarchical lattices can be generated by recursively applying an “inflation” operation whereby each edge is expanded into a cell having  $b$  parallel branches of length  $s$ . Renormalization on these lattices can be done exactly. For the purpose of this discussion, consider the case where  $b = s = 3$ . When the distribution of couplings is continuous, one has  $\theta \approx -0.278$ , while when using the  $\pm J$  distribution one has  $\theta = 0$ . Indeed, there are *two* fixed point distributions of the couplings: a generic (continuous) one for which the energy scale goes to zero ( $\theta < 0$ ) and another one which is very special, being a sum of delta functions on odd integers (and leading to  $\theta = 0$ ).

Now what happens when we turn on the temperature in this real space RG framework? At very low  $T$ , one is very close to the critical manifold, so the renormalization will first flow toward one of the  $T = 0$  fixed points; the corresponding fixed point determines the critical exponents of the system. In the case of the  $\pm J$  model, the initial distribution starts by being nearly concentrated on odd integers. However, as we increase the lattice size, this initial distribution will be less and less of that form: The iterations renormalize the *free* energy  $F = E - TS$ , and, since  $S$  fluctuates, we lose the quantization property rapidly with size. The flow is thus toward the “continuous” distribution fixed point for which  $\theta < 0$ . In Fig. 5, we display the specific heat as a function of  $T$  for this  $\pm J$  model; as expected, the behavior indicates a power scaling of  $c_v$  totally compatible with the value of  $\alpha$  obtained from the continuous distribution fixed point.

*Summary and conclusions.*—In this study of two-dimensional SG, we examined the effect of the underlying distribution of couplings on the critical thermodynamics. We found several remarkable behaviors: (1)  $\eta$  is model insensitive and very close to zero in all models. (2) The divergence of  $\xi$  does not seem to depend on the model, and the corresponding exponent is given by  $\nu = -1/\theta$  as long

as one uses the  $\theta$  of the continuous models. (3) The specific heat exponent  $\alpha$  can be measured using the discrete models, whereas in the continuous models this singularity is subdominant and, thus, numerically inaccessible. Hyperscaling is consistent with the data.

From our observations, we conclude that thermal properties of 2D SG fall into a single universality class. This is in contrast to what happens exactly at  $T = 0$ : There, an additional fixed point of the RG arises, allowing different scaling in the continuous and in the  $\pm J$  type models.

This work was supported by the EEC’s FP6 IST Programme under Contract No. IST-001935, EVERGROW, and by the EEC’s HPP under Contracts No. HPRN-CT-2002-00307 (DYGLAGEMEM) and No. HPRN-CT-2002-00319 (STIPCO). The LPTMS is an Unité de Recherche de l’Université Paris XI associée au CNRS.

- 
- [1] M. Mézard, G. Parisi, and M. A. Virasoro, *Spin-Glass Theory and Beyond* (World Scientific, Singapore, 1987).
  - [2] C. Amoruso, E. Marinari, O. C. Martin, and A. Pagnani, *Phys. Rev. Lett.* **91**, 087201 (2003).
  - [3] D. S. Fisher and D. A. Huse, *Phys. Rev. Lett.* **56**, 1601 (1986).
  - [4] A. J. Bray and M. A. Moore, *Phys. Rev. Lett.* **58**, 57 (1987).
  - [5] H. Katzgraber, L. Lee, and A. Young, *Phys. Rev. B* **70**, 014417 (2004).
  - [6] J. Houdayer and A. Hartmann, *Phys. Rev. B* **70**, 014418 (2004).
  - [7] R. H. Swendsen and J.-S. Wang, *Phys. Rev. Lett.* **58**, 86 (1987).
  - [8] J. Houdayer, *Eur. Phys. J. B* **22**, 479 (2001).
  - [9] J. Lukic *et al.*, *Phys. Rev. Lett.* **92**, 117202 (2004).
  - [10] H. Katzgraber and L. Lee, *Phys. Rev. B* **71**, 134404 (2005).
  - [11] S. F. Edwards and P. W. Anderson, *J. Phys. F* **5**, 965 (1975).
  - [12] R. H. Swendsen and J.-S. Wang, *Phys. Rev. Lett.* **57**, 2607 (1986).
  - [13] K. Hukushima and K. Nemoto, *J. Phys. Soc. Jpn.* **65**, 1604 (1996).
  - [14] A. Galluccio, M. Loebl, and J. Vondrák, *Phys. Rev. Lett.* **84**, 5924 (2000).
  - [15] S. Caracciolo *et al.*, *Phys. Rev. Lett.* **74**, 2969 (1995).
  - [16] M. Palassini and S. Caracciolo, *Phys. Rev. Lett.* **82**, 5128 (1999).
  - [17] H.-F. Cheung and W. L. McMillan, *J. Phys. C* **16**, 7027 (1983).
  - [18] H.-F. Cheung and W. L. McMillan, *J. Phys. C* **16**, 7033 (1983).
  - [19] G. A. Baker and J. C. Bonner, *Phys. Rev. B* **12**, 3741 (1975).
  - [20] J. Lukic, E. Marinari, and O. C. Martin, *Europhys. Lett.* **73**, 779 (2006).
  - [21] B. W. Southern and A. Young, *J. Phys. C* **10**, 2179 (1977).